Inorg. Chem. **2003**, *42*, 2783–2788

Dinuclear Iron(II)–Cyanocarbonyl Complexes Linked by Two/Three Bridging Ethylthiolates: Relevance to the Active Site of [Fe] Hydrogenases

Wen-Feng Liaw,*,† Wen-Ting Tsai,‡ Hung-Bin Gau,‡ Chien-Ming Lee,† Shin-Yuan Chou,‡ Wen-Yuan Chen,‡ and Gene-Hsiang Lee§

Department of Chemistry, Naional Tsing Hua University, Hsinchu 30043, Taiwan, Department of Chemistry, National Changhua University of Education, Changhua 50058, Taiwan, and Instrumentation Center, National Taiwan University, Taipei 10764, Taiwan

Received October 22, 2002

Dinuclear iron(II)–cyanocarbonyl complex $[PPN]_2[Fe(CN)_2(CO)_2(\mu\text{-SEt})]_2$ (**1**) was prepared by the reaction of [PPN]-$[FeBr(CN)_2(CO)_3]$ and [Na][SEt] in THF at ambient temperature. Reaction of complex **1** with [PPN][SEt] produced the triply thiolate-bridged dinuclear Fe(II) complex $[PPN][(CN)(CO)_2Fe(\mu\text{-SEt})_3Fe(CO)_2(CN)]$ (**2**) with the torsion angle of two CN^- groups (C(5)N(2) and C(3)N(1)) being 126.9°. The extrusion of two σ-donor CN^- ligands from Fe(II)Fe(II) centers of complex **1** as a result of the reaction of complex **1** and [PPN][SEt] reflects the electron-rich character of the dinuclear iron(II) when ligated by the third bridging ethylthiolate. The Fe–S distances (2.338(2) and 2.320(3) Å for complexes **1** and **2**, respectively) do not change significantly, but the Fe^{II}–Fe^{II} distance contracts from 3.505 Å in complex **1** to 3.073 Å in complex **2**. The considerably longer Fe^{II}–Fe^{II} distance of 3.073 Å in complex **2**, compared to the reported Fe–Fe distances of 2.6/2.62 Å in DdHase and CpHase, was attributed to the presence of the third bridging ethylthiolate, instead of π-accepting CO-bridged ligand as observed in [Fe] hydrogenases. Additionally, in a compound of unusual composition $\{[Na^{\bullet 5}/_2H_2O][(CN)(CO)_2Fe(\mu\text{-SEt})_3Fe(CO)_2(CN)]\}_n\{^1/_2O(Et)_2\}_n$ (**3**), the Na^+ cations and H_2O molecules combining with dinuclear $[(CN)(CO)_2Fe(\mu\text{-SEt})_3Fe(CO)_2(CN)]^-$ anions create a polymeric framework wherein two CN^- ligands are coordinated via CN^-–Na^+/CN^-–$(Na^+)_2$ linkages, respectively.

Introduction

Hydrogen metabolism (reversibly catalyzed H_2 molecules) in the biological energy cycle is mostly mediated by two types of metal-containing enzymes, [Fe]-only hydrogenases and [NiFe] hydrogenases.[1,2] The recent report of high-quality X-ray crystal structures of [Fe]-only hydrogenases isolated from *Desulfovibrio desulfuricans* (DdHase)/*Clostridium pasteurianum* (CpHase) revealed that the active sites are composed of a conventional [4Fe−4S] subcluster linked by a bridging cysteine to a dinuclear iron subcluster.[3−6] The crystal structures,[3−6] in combination with FTIR data,[6] suggest that the dinuclear iron subcluster is ligated by terminal CO and CN^- diatomic molecules with the two iron atoms linked by a di(thiomethyl)-amine ligand (DdHase)/two thiolate ligands (CpHase) and a carbonyl group (DdHase). Upon reduction, FTIR spectra and the crystal structure show that the previously bridging CO shifts toward the distal iron that most likely serves as the primary hydrogen binding site.[6]

Studies on the electronic structure of the active center of [Fe]-only hydrogenases may provide insight into understanding the catalytic mechanism of [Fe] hydrogenases. Mössbauer study of the H cluster in [Fe] hydrogenases isolated from *C. pasteurianum* (CpII) showed that the dinuclear Fe subcluster

* Author to whom correspondence should be addressed. E-mail: wfliaw@mx.nthu.edu.tw.
† Naional Tsing Hua University.
‡ National Changhua University of Education.
§ National Taiwan University.

(1) (a) Adams, M. W. W. *Biochim. Biophys. Acta* **1990**, *1020*, 115. (b) Nicolet, Y.; Lemon, B. J.; Fontecilla-Camps, J. C.; Peters, J. W. *Trends Biochem. Sci*. **2000**, *25*, 138. (c) Peters, J. W. *Curr. Opin. Struct. Biol*. **1999**, *9*, 670.
(2) (a) Albracht, S. P. J. *Biochim. Biophys. Acta* **1994**, *1178*, 167. (b) Volbeda, A.; Charon, M. H.; Piras, C.; Hatchikian, E. C.; Frey, M.; Fontecilla-Camps, J. C. *Nature* **1995**, *373*, 580.
(3) Peters, J. W.; Lanzilotta, W. N.; Lemon, B. J.; Seefeldt, L. C. *Science* **1998**, *282*, 1853.
(4) Nicolet, Y.; Piras, C.; Legrand, P.; Hatchikian, C. E.; Fontecilla-Camps, J. C. *Structure* **1999**, *7*, 13.
(5) (a) Lemon, B. J.; Peters, J. W. *J. Am. Chem. Soc.* **2000**, *122*, 3793. (b) Lemon, B. J.; Peters, J. W. *Biochemistry* **1999**, *38*, 12970.
(6) Nicolet, Y.; de Lacey, A. L.; Vernéde, X.; Fernandez, V. M.; Hatchikian, E. C.; Fontecilla-Camps, J. C. *J. Am. Chem. Soc*. **2001**, *123*, 1596.

10.1021/ic0261225 CCC: $25.00
Published on Web 03/26/2003

contains two low-spin $Fe^{II}-Fe^{II}$ sites in the reduced state (H_{red}), while it is in the mixed-valence $Fe^{III}-Fe^{II}$ site in the oxidized state (H_{ox} and H_{ox}-CO).[7] In contrast, Nicolet et al. argued that in the oxidized active state of the H cluster, the Fe ions of the dinuclear subcluster could be either in ferrous intermediate spin ($S = 1$) or ferric low spin ($S = {}^1/_2$).[6] Recent studies implicate that $Fe^{I}-Fe^{I}$ forms are also possible in the dinuclear iron subcluster of the active-site of [Fe] hydrogenases since the $Fe^{I}-Fe^{I}$ distance of 2.517(12) Å in (μ-pdt)-$[Fe(CO)_2(CN)]_2^{2-}$ (pdt = $SCH_2CH_2CH_2S$)[8] is closely comparable with the Fe−Fe distance of 2.6 and 2.62 Å observed in [Fe] hydrogenases isolated from *D. desulfuricans* and *C. pasteurianum*.[3,4] The Fe−Fe distance of 2.6/2.62 Å observed in DdHase and CpHase is significantly different from the $Fe^{II}-Fe^{II}$ distance of 3.473 Å found in $[Fe(CO)_2(CN)(-SC_6H_4S-)]_2^{2-}$,[9] but comparable to that observed in (μ-H)(μ-pdt)$[Fe(CO)_2(PMe_3)]_2^+$ (2.578(1) Å), a functional model of [Fe] hydrogenases in the catalytic isotopic scrambling of D_2/H_2O and H_2/D_2 mixtures.[10,11] In particular, the recent discovery by Rauchfuss and co-workers shows that $[HFe_2(\mu\text{-}SR)_2(CO)_4(CN)(PMe_3)]$ serves as a catalyst for proton reduction.[12]

Very recently, De Lacey et al. obtained high-quality FTIR spectra for the H_{ox} and the CO-inhibited H_{ox} (H_{ox}-CO) from DdHase and indicated that the H_{ox} and the H_{ox}^{air} (fully oxidized, inactive state) have similar structures.[13] Inspection of the ν_{CO} stretching frequencies (1965, 1940, 1802 cm^{-1}) of the H_{ox} form of DdHase[13] reveals that these bands are significantly different from those of the Fe(II) bioorganometallic complex $[Fe(CO)_2(CN)(-SC_6H_4S-)]_2^{2-}$ (2011, 1961 cm^{-1}).[6,9] The distinct differences in ν_{CO} between (μ-pdt)$[Fe^{I}(CO)_2(CN)]_2^{2-}$ (1964, 1924, 1885 cm^{-1})[8,11] and [Fe] hydrogenases isolated from *D. desulfuricans* (2016, 1972, 1963, 1811 cm^{-1}, CO-inhibited form)[6,13] suggest the distinguishable electronic structure of the iron atoms in the model compound (μ-pdt)-$[Fe(CO)_2(CN)]_2^{2-}$ and the CO-inhibited DdHase (CO is known to be a reliable reporter ligand for electron density changes). The inconsistency between the observed $Fe^{I}-Fe^{I}$ distance and the low-spin $Fe^{II}-Fe^{II}$ assignment was noted in the studies of the dinuclear iron−cyanocarbonyl−thiolate model compounds and the Mössbauer spectra of *C. pasteurianum* enzyme, respectively.[4,6,7,9,10] Obviously, the oxidation states of the diiron subcluster in different redox forms of [Fe] hydrogenase are still controversial,[13,14] although it is generally believed that the dinuclear Fe subcluster of DdHase and CpHase may be assigned as $[Fe^{II}Fe^{II}]$, $[Fe^{I}Fe^{II}]$, and $[Fe^{I}-Fe^{I}]$ in the fully oxidized (inactive), the oxidized (active), and the reduced states, respectively.[6,13,14]

Scheme 1

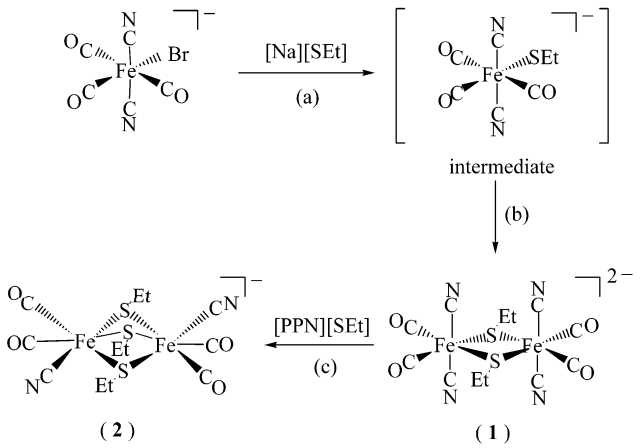

Here we report two dinuclear iron−thiolate cyanocarbonyl compounds, $[Fe(CN)_2(CO)_2(\mu\text{-}SEt)]_2^{2-}$ (**1**) and $[Fe_2(CN)_2(CO)_4(\mu\text{-}SEt)_3]^-$ (**2**). The coordination chemistry of complexes **1** and **2** suggests that the certain total number of thiolate and cyanide ligands coordinated to Fe(II) center provides significant stabilization to the dinuclear Fe(II)−carbonyl complexes and reveals the significant $Fe^{II}-Fe^{II}$ distance contraction as the dinuclear iron(II)−cyanocarbonyl complex is transformed from the doubly thiolate-bridged to the triply thiolate-bridged forms. On the basis of IR ν_{CO} stretching frequencies of complexes **1** and **2**, these results may provide insights into the electronic features of the dinuclear iron subcluster of the [Fe] hydrogenase active site.

Results and Discussion

When $[PPN][Fe(Br)(CN)_2(CO)_3]]$ (0.5 mmol)[15] was reacted directly with [Na][SEt] (0.5 mmol) in THF at room temperature, dinuclear hexacoordinate d^6 Fe^{II} complex $[PPN]_2[Fe(CN)_2(CO)_2(\mu\text{-}SEt)]_2$ (**1**) was isolated as light yellow crystals after recrystallization from THF−hexane (yield 18%) (Scheme 1a,b). A nucleophilic displacement and the concomitant dimerization may account for the formation of complex **1**. Attempts to detect the extremely unstable intermediate, the mononuclear $[Fe(CN)_2(CO)_3(SEt)]^-$, by FTIR were unsuccessful (Scheme 1a). The IR spectrum of complex **1** in the aprotic solvent CH_3CN reveals two weak absorption bands for the CN^- ligands at 2121 vw, 2108 w cm^{-1} supporting a trans position of two CN^- groups, while the two strong absorption bands 2033s, 1984 s cm^{-1} assigned to the carbonyl stretching frequencies support a cis position

(7) Popescu, C. V.; Münck, E. *J. Am. Chem. Soc.* **1999**, *121*, 7877.
(8) (a) Schmidt, M.; Contakes, S. M.; Rauchfuss, T. B. *J. Am. Chem. Soc.* **1999**, *121*, 9736. (b) Le Cloirec, A.; Best, S. P.; Borg, S.; Davies, S. C.; Evans, D. J.; Hughes, D. L.; Pickett, C. J. *Chem. Commun.* **1999**, 2285.
(9) Liaw, W.-F.; Lee, N.-H.; Chen, C.-H.; Lee, C.-M.; Lee, G.-H.; Peng, S.-M. *J. Am. Chem. Soc.* **2000**, *122*, 488.
(10) (a) Zhao, X.; Georgakaki, I. P.; Miller, M. L.; Yarbrough, J. C.; Darensbourg, M. Y. *J. Am. Chem. Soc.* **2001**, *123*, 9710. (b) Darensbourg, M. Y.; Lyon, E. J.; Smee, J. J. *Coord. Chem. Rev.* **2000**, *206*, 533.
(11) (a) Lyon, E. J.; Georgakaki, I. P.; Reibenspies, J. H.; Darensbourg, M. Y. *Angew. Chem., Int. Ed.* **1999**, *38*, 3178. (b) Lyon, E. J.; Georgakaki, I. P.; Reibenspies, J. H.; Darensbourg, M. Y. *J. Am. Chem. Soc.* **2001**, *123*, 3268.
(12) Gloaguen, F.; Lawrence, J. D.; Rauchfuss, T. B. *J. Am. Chem. Soc.* **2001**, *123*, 9476.
(13) De Lacey, A. L.; Stadler, C.; Cavazza, C.; Hatchikian, E. C.; Fernandez, V. M. *J. Am. Chem. Soc.* **2000**, *122*, 11232.
(14) (a) Pierik, A. J.; Hulstein, M.; Hagen, W. R.; Albracht, S. P. *Eur. J. Biochem.* **1998**, *258*, 572. (b) Patil, D. S.; Moura, J. J. G.; He, S. H.; Teixeira, M.; Prickril, B. C.; Der Vartanian, D. V.; Peck, H. D., Jr.; Legall, J.; Huyanh, B. H. *J. Biol. Chem.* **1988**, *263*, 18732. (c) Cao, Z. X.; Hall, M. B. *J. Am. Chem. Soc.* **2001**, *123*, 3734. (d) Liu, Z.-P.; Hu, P. *J. Am. Chem. Soc.* **2002**, *124*, 5175.
(15) Liaw, W.-F.; Lee, J.-H.; Gau, H.-B.; Chen, C.-H.; Jung, S.-J.; Hung, C.-H.; Chen, W.-Y.; Hu, C.-H.; Lee, G.-H. *J. Am. Chem. Soc.* **2002**, *124*, 1680.

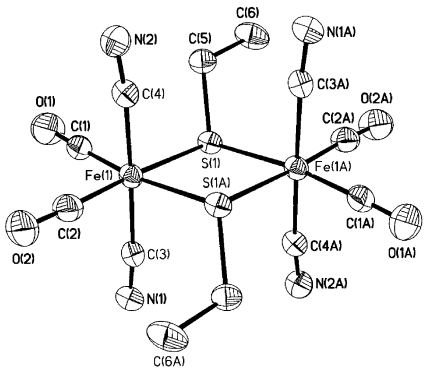

Figure 1. ORTEP drawing and labeling scheme of the $[(CN)_2(CO)_2Fe(\mu\text{-}SEt)]_2^{2-}$ anion.

Table 1. Selected Bond Distances (Å) and Angles (deg) for Complexes (a) **1** and (b) **2**

		Complex **1**	
Fe(1)−C(1)	1.762(7)	Fe(1)−C(2)	1.777(6)
Fe(1)−C(3)	1.924(6)	Fe(1)−C(4)	1.926(6)
Fe(1)−S(1)	2.3462(15)	Fe(1)−S(1A)	2.3291(16)
C(1)−Fe(1)−C(2)	94.3(3)	C(3)−Fe(1)−C(4)	176.4(2)
S(1)−Fe(1)−S(1A)	82.86(5)	Fe(1)−S(1)−Fe(1A)	97.14(5)
		Complex **2**	
Fe(1)−C(1)	1.786(9)	Fe(1)−C(2)	1.745(9)
Fe(1)−C(3)	1.945(10)	Fe(1)−S(3)	2.318(3)
Fe(1)−S(2)	2.318(3)	Fe(1)−S(1)	2.324(2)
Fe(2)−C(4)	1.766(11)	Fe(2)−C(6)	1.767(10)
Fe(2)−C(5)	1.954(9)	Fe(2)−S(1)	2.317(3)
Fe(2)−S(3)	2.324(2)	Fe(2)−S(2)	2.330(3)
C(1)−Fe(1)−C(2)	94.0(4)	C(2)−Fe(1)−C(3)	88.7(4)
C(1)−Fe(1)−C(3)	87.4(4)	C(2)−Fe(1)−S(3)	173.2(3)
C(1)−Fe(1)−S(3)	92.5(3)	C(3)−Fe(1)−S(3)	93.6(3)
S(2)−Fe(1)−S(1)	81.47(9)	Fe(1)−S(2)−Fe(2)	82.78(9)

of two CO ligands (vibrationally uncoupled CO groups and CN^- groups on adjacent iron(II) sites).[9] The $Fe^{II}-Fe^{II}$ distance of 3.505 Å in complex **1** is considerably longer than those reported for the dinuclear iron subcluster (2.6 and 2.62 Å) of the [Fe] hydrogenase active site (Figure 1).[3,4] Here the lack of the third bridging CO ligand and the nearly square planar FeS_2Fe core in complex **1**, in contrast to butterfly structure of the active-site FeS_2Fe core observed in [Fe] hydrogenases,[3,4] are adopted to rationalize the significantly longer $Fe^{II}-Fe^{II}$ distance in complex **1**. Presumably, the role of increments of CN^- ligands coordinated to the Fe(II)Fe(II) center in complex **1**, compared to dinuclear Fe(I)Fe(I) compound $(\mu\text{-pdt})[Fe^I(CO)_2(CN)]_2^{2-}$,[8,11] is to increase the electron density in the $Fe^{II}-Fe^{II}$ center as well as to stabilize the $Fe^{II}-Fe^{II}$ oxidation level.

Selected bond distances and angles are given in Table 1. The dinuclear $[Fe(CN)_2(CO)_2(\mu\text{-}SEt)]_2^{2-}$ is electronically dianionic, and therefore both irons should be divalent. Complex **1** exhibits a diagnostic ^1H NMR spectrum with the ethylthiolate proton resonances at 2.698 (q), 1.270 (t) ppm, which are consistent with the Fe(II) having a low-spin d^6 electronic configuration in an octahedral ligand field. Complex **1** possesses crystallographically imposed centrosymmetry. Each iron atom is surrounded pseudooctahedrally by two bridging ethylthiolates, two cyanides, and two carbonyl groups, and two pairs of CN groups (C(4)N(2), C(4A)N(2A) and C(3)N(1), C(3A)N(1A)) point into the antiparallel direction. Formation of complex **1** can be interpreted as coordinative association of two five-coordinate electron-deficient mononuclear $[Fe(CN)_2(CO)_2(SEt)]^-$, and attributed to the instability of the monomeric $[Fe(CN)_2(CO)_2(SEt)]^-$ as well as the avoidance of electron deficiency at the monomeric iron(II) centers. The average Fe−CO and Fe−CN bond lengths are 1.769(7) and 1.925(6) Å, respectively.

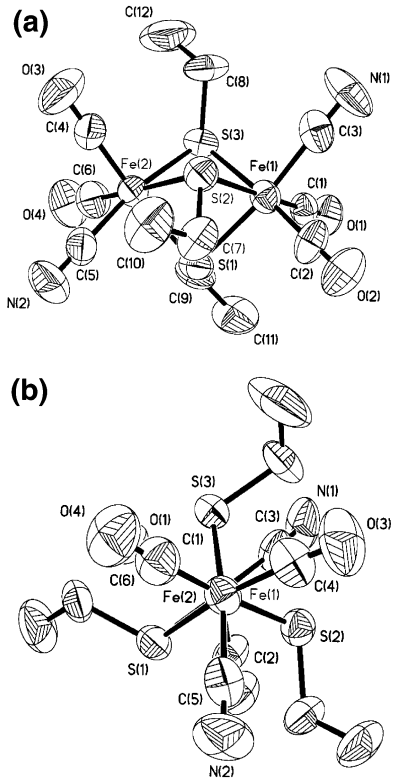

Figure 2. (a) ORTEP drawing and labeling scheme of the $[(CN)(CO)_2Fe(\mu\text{-}SEt)_3Fe(CO)_2(CN)]^-$ anion. (b) A view along the Fe(2)−Fe(1) axis for the $[(CN)(CO)_2Fe(\mu\text{-}SEt)_3Fe(CO)_2(CN)]^-$ anion. Hydrogen atoms are omitted for clarity. Torsion angles (deg): C(4)−Fe(2)−Fe(1)−C(3), 10.5; C(5)−Fe(2)−Fe(1)−C(3), 126.9; C(5)−Fe(2)−Fe(1)−C(2), 10.0; C(6)−Fe(2)−Fe(1)−C(1), 0.5.

Subsequent reactions of complex **1** with [PPN][SEt] in a 1:1 molar ratio in THF produced the thermally stable $[PPN][Fe_2(CN)_2(CO)_4(\mu\text{-}SEt)_3]$ (**2**) (yield 23%), and the known *trans*-$[PPN]_2[Fe(CN)_4(CO)_2]$ (**3**) (yield 8%)[15,16] as identified by IR and X-ray diffraction (Scheme 1c). Obviously, the transformation of complex **1** into complex **2** is accompanied by extrusion of two σ-donor CN^- ligands from iron(II) centers of complex **1**, reflecting the electron-rich character of the dinuclear iron(II) when ligated by the third bridging ethylthiolate. That is, the nucleophilic reaction of [PPN][SEt] occurs at the more electron-deficient iron(II) site to yield complex **2**. Structurally, the Fe−S distances (2.338(2) Å (average) for complex **1** and 2.320(3) Å (average) for complex **2**) do not change significantly, but the $Fe^{II}-Fe^{II}$ distance decreases from 3.505 Å in complex **1** to 3.073 Å in complex **2**, and this shortening of the $Fe^{II}-Fe^{II}$ distance in complex **2** is accompanied by a decrease in the ∠Fe−S−Fe angles from 97.14(5)° to 82.88(9)° (Figure 2) (Table 1). The $Fe^{II}-$

(16) Jiang, J.; Koch, S. A. *Angew. Chem., Int. Ed.* **2001**, *40*, 2629.

Fe^{II} distance of 3.073 Å in complex **2** is considerably longer than the $Fe^{I}-Fe^{I}$ distance of 2.5090(6) Å in (μ-SCH_2NMeCH_2S-)$[Fe(CO)_2(CN)]_2^{2-}$,[18] but comparable to the $Fe^{II}-Fe^{II}$ distance of 3.07 Å observed in $[(PR_3)(CO)_2Fe(\mu\text{-}SR)_3Fe(CO)_2(PR_3)]^+$ (R = alkyl).[19] Two Fe(II) atoms are connected via three thiolate bridges, and the ethyl groups of three bridging μ_2-ethylthiolates in **2** form a regular propeller-like arrangement around the S_3 plane defined by the three sulfurs (Figure 2). Two groups, $[Fe(1)(CO)_2(CN)]$ and $[Fe(2)(CO)_2(CN)]$, are in an eclipsed conformation with the torsion angle of two CN^- groups (C(5)N(2) and C(3)N(1)) being 126.9° (Figure 2b). The average Fe−CO and Fe−CN bond lengths of 1.766(11) and 1.950(10) Å, respectively, closely compare with those found in complex **1** (1.769(7) and 1.925(6) Å, respectively) (Table 1).

The anionic complex **2** exhibits a one-band pattern in the ν_{CN} region (2110 w cm^{-1} (THF)) and a three-band pattern in the ν_{CO} region (2029 w, 2014 s, 1968 m cm^{-1} (THF)), similar to the ν_{CN} and ν_{CO} spectra (ν_{CN} 2108; ν_{CO} 2048, 2024, 1987 cm^{-1}) of (μ-H)(μ-pdt)$[Fe^{II}(CO)_2(CN)]_2^-$ reported recently by Darensbourg and co-workers.[10,11] Obviously, the ν_{CO} stretching frequencies of complex **2** are much higher, compared to those of the fully reduced state (H_{red}) (1965, 1940, 1916, 1894 cm^{-1}) of the dinuclear iron subcluster of DdHase.[1,13,14] If complex **2** and the H_{ox}-CO DdHase have the same oxidation level for dinuclear iron, one would expect that the dinuclear iron active site of the H cluster shows higher ν_{CO} stretching frequencies than complex **2**, since the third bridging $[SEt]^-$ ligand of complex **2** is a better electron donor than a bridging CO group observed in H_{ox}-CO DdHase, except that the $[Fe_4S_4]$-S_{cys} unit serves as a stronger electron donor. However, the ν_{CO} vibrational frequencies of the triply ethylthiolate-bridged complex **2** are even higher than those of the H_{ox}-CO DdHase (2016, 1972, 1963, 1811 cm^{-1}), of which the lowest band at 1811 cm^{-1} was assigned to be the stretching mode of bridging CO in the H cluster.[6,13,14] This result may lend support for the H_{ox}-CO and H_{ox} (active) states of DdHase, showing the ν_{CO} stretching bands at 2016, 1972, 1963, 1811 cm^{-1} and 1965, 1940, 1802 cm^{-1}, respectively, being the mixed-valent Fe(II)−Fe(I), a prominent candidate responsible for H_2 uptake, heterolytic cleavage of H_2.[6,13,14] Alternatively, THF solution of a mixture of $[PPN][Fe(CO)_4(CN)]$ (0.5 mmol) and I_2 (0.5 mmol) was added to [Na][SEt] (1 mmol) and stirred under N_2 at 25 °C. The reaction mixture finally led to the isolation of an orange solid, which was recrystallized from diethyl ether−hexane as orange crystals of $\{[Na^{\bullet 5/2}H_2O][(CN)(CO)_2Fe(\mu\text{-}SEt)_3Fe(CO)_2(CN)]\}_n\{^1/_2O(Et)_2\}_n$ (**3**). The compound of unusual composition, $\{[Na^{\bullet 5/2}H_2O][(CN)(CO)_2Fe(\mu\text{-}SEt)_3Fe(CO)_2(CN)]\}_n\{^1/_2O(Et)_2\}_n$, is a polymer containing dinuclear $[(CN)(CO)_2Fe(\mu\text{-}SEt)_3Fe(CO)_2(CN)]$ units connected through $CN^-\cdots Na^+(H_2O)_2$ interactions to form layers (chains). The polymeric orange solid is insoluble in noncoordinating solvents, such as hexane and CH_2Cl_2, but shows good solubility in diethyl ether and THF, which allows one to perform the solution NMR experiments. In the ^1H NMR spectrum, a singlet for the H_2O molecules at δ 2.47 ppm is observed. Three sharp quartet (δ 2.33, 2.50, 2.71 ppm) and two triplet (δ 1.30, 1.48 ppm) ^1H NMR resonances were assigned to three nonequivalent $-SCH_2CH_3$ groups in C_4D_8O solution. On the basis of solubility and ^1H NMR spectroscopy, it is assumed that the structural feature (polymeric structure) found for complex **3** in the solid state is retained with tetrahydrofuran molecules displacing H_2O molecules and coordinating to Na^+ cations in THF, although we cannot unambiguously rule out the possibility of formation of the monomeric dinuclear complex $[Na^{\bullet}(THF\text{-}H_2O)_n][(CN)(CO)_2Fe(\mu\text{-}SEt)_3Fe(CO)_2(CN)]$ in THF solution. Treatment of complex **3** with [PPN][Cl] in THF for 1 h results in an infrared ν_{CN}/ν_{CO} spectrum identical with that of complex **2** (ν_{CN}/ν_{CO} shift from 2120 w, 2113 w, 2032 m, 2019 s, 1976 m to 2110 w, 2029 m, 2014 s, 1968 m cm^{-1} in THF).

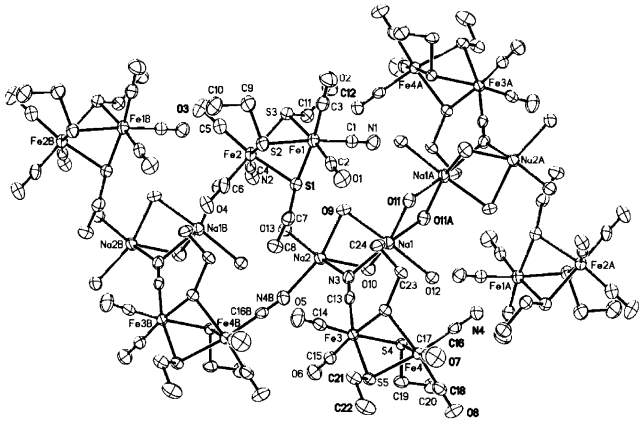

Figure 3. X-ray structural diagram of the three-dimensional lattice showing the interactions of Na cations with the $[(CN)(CO)_2Fe(\mu\text{-}SEt)_3Fe(CO)_2(CN)]^-$ anions and H_2O molecules in complex **3**.

The X-ray structural diagram of the three-dimensional lattice of complex **3** is shown in Figure 3. The Na cations and H_2O molecules combine with the homodinuclear $[(CN)(CO)_2Fe(\mu\text{-}SEt)_3Fe(CO)_2(CN)]^-$ anions to create a polymeric framework wherein two CN ligands are coordinated via $CN-Na^+/CN-(Na^+)_2$ linkages (i.e., one cyanide group ligated Fe and Na cation as $Fe-CN-Na^+$ while the other cyanide group ligated to one Fe and two Na cations by $Fe-CN-(Na^+)_2$), respectively. The Na cations occur in pairs linked by two bridging H_2O molecules and one CN group, and the inter-pairs of Na cations are linked by two H_2O molecules. Also, each Na^+ center is additionally coordinated to one terminal H_2O ligand. The Fe−CO distances (1.775(5) Å, average) and Fe−CN distances (1.912(4) Å, average) are consistent with those in complex **2** (Table 2). The $Fe^{II}-Fe^{II}$ distance of 3.087 Å in complex **3** is longer than that in complex **2**. Two fragments, $Fe(3)(CO)_2(CN)$ and $Fe(4)(CO)_2(CN)$, are in an eclipsed conformation with the torsion angle of the two CN groups (C(13)N(3) and C(16)N(4)) being 3.5° (Figure 3).

(17) Rauchfuss, T. B.; Contakes, S. M.; Hsu, S. C. N.; Reynolds, M. A.; Wilson, S. R. *J. Am. Chem. Soc*. **2001**, *123*, 6933.
(18) Lawrence, J. D.; Li, H.; Rauchfuss, T. B.; Benard, M.; Rohmer, M.-M. *Angew. Chem., Int. Ed*. **2001**, *40*, 1768.
(19) (a) Treichel, P. M.; Crane, R. A.; Matthews, R.; Bonnin, K. R.; Powell, D. *J. Organomet. Chem*. **1991**, *402*, 233. (b) Schultz, A. J.; Eisenberg, R. *Inorg. Chem*. **1973**, *12*, 518.

Table 2. Selected Bond Distances (Å) and Angles (deg) for Complex **3**

Fe(1)−C(3)	1.765(5)	Fe(1)−C(2)	1.786(5)
Fe(1)−C(1)	1.909(4)	Fe(2)−C(5)	1.771(5)
Fe(2)−C(6)	1.778(5)	Fe(2)−C(4)	1.915(4)
Fe(1)−S(1)	2.3182(12)	Fe(1)−S(2)	2.3082(12)
Fe(1)−S(3)	2.3264(12)	Fe(2)−S(1)	2.3148(11)
Fe(2)−S(2)	2.3345(12)	Fe(2)−S(3)	2.3194(13)
Na(1)−N(3)	2.513(4)	Na(2)−N(3)	2.554(3)
Na(1)−O(12)	2.422(3)	Na(1)−O(9)	2.428(3)
Na(1)−Na(2)	3.177(2)	Na(2)−O(9)	2.343(3)
C(1)−Fe(1)−C(2)	91.45(18)	C(2)−Fe(1)−S(2)	94.94(14)
S(1)−Fe(1)−S(2)	80.53(4)	Fe(2)−S(1)−Fe(1)	83.19(4)
O(11)−Na(1)−O(10)	155.31(12)	O(11)−Na(1)−O(9)	87.63(10)
O(12)−Na(1)−N(3)	93.94(11)	O(9)−Na(1)−N(3)	82.18(11)
O(11)−Na(1)−Na(2)	131.83(9)	O(10)−Na(1)−Na(2)	46.37(7)
N(3)−Na(1)−Na(2)	51.75(8)	O(10)−Na(1)−N(3)	81.25(11)

Summary. Doubly and triply thiolate-bridged dinuclear iron(II)−cyanocarbonyl complexes $[PPN]_2[Fe(CN)_2(CO)_2(\mu\text{-SEt})]_2$ (**1**) and $[PPN][(CN)(CO)_2Fe(\mu\text{-SEt})_3Fe(CO)_2(CN)]$ (**2**) were prepared, respectively, by the reactions of $[PPN][FeBr(CN)_2(CO)_3]$ and [Na][SEt] in THF at ambient temperature. The extrusion of two strong σ-donor CN^- ligands from iron(II) centers of complex **1** as a result of the reaction of complex **1** and [PPN][SEt] reflects the electron-rich character of the dinuclear iron(II) when ligated by the third bridging ethylthiolate. Notably, the certain total number of thiolate and cyanide ligands coordinated to the Fe center (**1** vs **2** vs $(\mu\text{-pdt})[Fe(CO)_2(CN)]_2^{2-}$) stabilizes the binding of carbon monoxide to iron metals in the intermediate oxidation state.[8−12] The $Fe^{II}−Fe^{II}$ distance decreases from 3.505 Å in complex **1** to 3.073 Å in complex **2**. The considerably longer $Fe^{II}−Fe^{II}$ distance of 3.073 Å in complex **2**, compared to the reported Fe−Fe distances of 2.6/2.62 Å in [Fe] hydrogenases isolated from Dd and Cp,[3−5] can be attributed to the presence of the third bridging ethylthiolate, instead of π-accepting CO-bridged ligand as observed in [Fe] hydrogenases. Presumably, the dinuclear iron linked by two thiolates and one CO group observed in the active site of [Fe] hydrogenases is constructed to provide short a Fe−Fe distance (Fe−Fe interelectronic interaction) and to stabilize the dinuclear Fe subunit.

Experimental Section

Manipulations, reactions, and transfers of samples were conducted under nitrogen according to standard Schlenk techniques or in a glovebox (argon gas). Solvents were distilled under nitrogen from appropriate drying agents (diethyl ether from CaH_2; acetonitrile from $CaH_2−P_2O_5$; methylene chloride from P_2O_5; hexane and tetrahydrofuran (THF) from sodium−benzophenone) and stored in dried, N_2-filled flasks over 4 Å molecular sieves. Nitrogen was purged through these solvents before use. Solvent was transferred to the reaction vessel via stainless steel cannula under a positive pressure of N_2. The reagents iron pentacarbonyl, hexamethyl disilazane sodium salt, cyanogen bromide, bis(triphenylphosphoranylidene)ammonium chloride ([PPN][Cl]), and sodium ethylthiolate (Lancaster/Aldrich) were used as received. Compound $[PPN][Fe(CO)_4(CN)]$ was synthesized and characterized by published procedures.[20] Infrared spectra of the carbonyl ν(CO) and cyanide ν(CN) stretching frequencies were recorded on a Bio-Rad model FTS-185 spectrophotometer with sealed solution cells (0.1 mm) and KBr windows. ^{1}H NMR spectra were obtained on a Bruker model AC 200 spectrometer. UV/vis spectra were recorded on a Hewlett-Packard 71 spectrophotometer. Analyses of carbon, hydrogen, and nitrogen were obtained with a CHN analyzer (Heraeus).

Preparation of $[PPN]_2[(CN)_2(CO)_2Fe(\mu\text{-SEt})]_2$ (1). The compounds $[PPN][Fe(CO)_3(CN)_2(Br)]$ (0.5 mmol, 0.405 g)[15] and [Na][SEt] (0.5 mmol, 0.042 g) were dissolved in THF (10 mL) and stirred overnight at ambient temperature. The reaction mixture was then filtered to remove NaBr, and hexane (15 mL) was added to precipitate the air-stable, orange yellow solid $[PPN]_2[(CN)_2(CO)_2Fe(\mu\text{-SEt})]_2$ (**1**). The yellow crystals $[PPN]_2[(CN)_2(CO)_2Fe(\mu\text{-SEt})]_2$ (**1**) suitable for X-ray diffraction were obtained by vapor diffusion of hexane into a THF solution of complex **1** at −15 °C (yield 0.069 g, 18%). IR: 2124 vw, 2112 w (ν_{CN}), 2029 s, 1981 s (ν_{CO}) cm^{-1} (THF); 2121 vw, 2108 w (ν_{CN}), 2033 s, 1984 s (ν_{co}) cm^{-1} (CH_3CN). ^{1}H NMR (CD_3CN): δ 2.698 (q), 1.270 (t) ($O−CH_2−CH_3$) ppm. Absorption spectrum (THF) [λ_{max}, nm (ϵ, M^{-1} cm^{-1})]: 338 (4563). Anal. Calcd for $C_{92}H_{90}O_8N_6P_4S_2Fe_2$: C, 64.72; H, 5.31; N, 4.92. Found: C, 64.45; H, 5.93; N, 5.14.

Preparation of $[PPN][(CN)(CO)_2Fe(\mu\text{-SEt})_3Fe(CO)_2(CN)]$ (2). The compounds $[PPN][Fe(CO)_3(CN)_2(Br)]$ (0.6 mmol, 0.486 g),[15] [Na][SEt] (0.9 mmol, 0.0756 g), and [PPN][Cl] (0.3 mmol, 0.1724 g) were loaded into a flask, and then 10 mL of THF was added under positive N_2 at room temperature. (Alternatively, a THF solution (8 mL) of compound **1** (0.3 mmol, 0.459 g) was added to [PPN][SEt] (0.3 mmol, 0.180 g) under positive N_2 at ambient temperature.) The reaction mixture was then stirred at 30 °C for 10 days. The upper solution was transferred to another flask via cannula under a positive pressure of N_2, and hexane (15 mL) was added to precipitate the orange yellow solid $[PPN][(CN)(CO)_2Fe(\mu\text{-SEt})_3Fe(CO)_2(CN)]$ (**2**). To grow X-ray diffraction quality crystals, crystallization vials containing a concentrated THF solution of complex **2** were placed in a septum-sealed container surrounded by hexane. Upon standing at 0 °C for 3 weeks, orange yellow thin-layer crystals (0.069 g, 23%) of **2** formed. IR: 2110 w (ν_{CN}), 2029 w, 2014 s, 1968 s (ν_{CO}) cm^{-1} (THF); 2106 w (ν_{CN}), 2033 w, 2020 s, 1976 s (ν_{CO}) cm^{-1} (CH_3CN). ^{1}H NMR (CD_3CN): δ 1.43 (t), 1.37 (t), 1.34 (t) ppm ($−CH_3$); 2.70−2.31 (m) ppm ($−CH_2−$). Absorption spectrum (THF) [λ_{max}, nm (ϵ, M^{-1} cm^{-1})]: 335 (2450). Anal. Calcd for $C_{48}H_{45}O_4N_3P_2S_3Fe_2$: C, 57.79; H, 4.54; N, 4.21. Found: C, 57.63; H, 4.38; N, 3.83. The residue was dried under vacuum and then redissolved in 8 mL of CH_3CN. The yellow solution was then filtered through Celite to remove NaBr and NaCl, and diethyl ether (15 mL) was added to precipitate the light yellow solid *trans*-$[PPN]_2[Fe(CN)_4(CO)_2]$ (0.032 g, 8%) identified by IR and X-ray diffraction. IR: 2105 m (ν_{CN}), 2004 s (ν_{CO}) cm^{-1} (CH_3CN).[16,17]

Preparation of $\{[Na\cdot{}^5/_2H_2O][(CN)(CO)_2Fe(\mu\text{-SEt})_3Fe(CO)_2(CN)]\}_n\{{}^1/_2O(Et)_2\}_n$ (3). A THF solution (6 mL) containing 0.368 g (0.5 mmol) of $[PPN][Fe(CO)_4(CN)]$ and 0.13 g (0.5 mmol) of I_2 in THF (6 mL) was stirred at room temperature for 2 h. The reaction was monitored immediately by IR. The spectrum (IR (THF): 2122 w (ν_{CN}), 2089 m, 2047 sh, 2093 s (ν_{CO}) cm^{-1}) was assigned to the formation of $[PPN][Fe(CO)_3(CN)(I)_2]$. In the same flask, 1 mmol of [Na][SEt] (0.094 g) was added, followed by stirring at room temperature for 2 days, and then diethyl ether (6 mL)−hexane (4 mL) was added to precipitate the byproducts (NaI, [PPN][I], and presumably [PPN][SEt]). The reaction mixture was filtered, and the orange-brown filtrate was dried under vacuum to afford the product. Diethyl ether (10 mL) was then added to extract the pure product $\{[Na\cdot{}^5/_2H_2O][(CN)(CO)_2Fe(\mu\text{-SEt})_3Fe(CO)_2(CN)]\}_n\{{}^1/_2O(Et)_2\}_n$ (**3**). Diffusion of hexane into a solution of complex **3** in

(20) (a) Ruff, J. K. *Inorg. Chem.* **1969**, *8*, 86. (b) Goldfield, S. A.; Raymond, K. N. *Inorg. Chem.* **1974**, *13*, 770.

Table 3. Crystallographic Data of Complexes (a) **1**, (b) **2**, and (c) **3**

	1·2H_2O·2THF	**2**	**3**
chem formula	$C_{92}H_{90}N_6O_8P_4S_2Fe_2$	$C_{48}H_{45}N_3O_4P_2S_3Fe_2$	$C_{28}H_{50}S_6Fe_4O_{14}Na_2N_4$
fw	1707.40	997.69	1128.46
cryst syst	monoclinic	monoclinic	monoclinic
space group	$P2_1/n$	$P2_1/c$	$P2_1/c$
λ, Å (Mo Kα)	0.7107	0.7107	0.7107
a, Å	10.7955(8)	10.9062(12)	9.5187(5)
b, Å	12.2741(8)	13.1631(14)	18.2710(8)
c, Å	32.795(2)	34.002(4)	28.4457(14)
α, deg	90	90	90
β, deg	95.903(2)	97.193(2)	99.0553 (9)
γ, deg	90	90	90
V, Å^3	4322.5(5)	4842.8(9)	4885.5(4)
Z	2	4	4
d_{calcd}, g cm^{-3}	1.312	1.368	1.534
μ, mm^{-1}	0.517	0.840	1.496
T, K	150(1)	293(2)	150(1)
R	0.0599[a]	0.0449[a]	0.0453[a]
R_{WF^2}	0.1142[b]	0.0839[b]	0.0717[b]
GOF	1.011	1.000	0.837

[a] $R = \sum|(F_o - F_c)|/\sum F_o$. [b] $R_{WF^2} = \{\sum w(F_o^2 - F_c^2)^2/\sum[w(F_o^2)^2]\}^{1/2}$.

diethyl ether at −15 °C for 4 weeks led to orange crystals (yield 48%, 0.073 g) suitable for X-ray crystallography. IR: 2123 w (ν_{CN}), 2036 m, 2023 s, 1981 m (ν_{CO}) (diethyl ether); 2120 w, 2112 w (ν_{CN}), 2033 m, 2018 s, 1975 m (ν_{CO}) (THF). ^{1}H NMR (C_4D_8O): δ 1.30 (t), 1.48 (t), 2.33 (q), 2.50 (q), 2.71 (q) ppm ($-SCH_2CH_3$); 2.47 (s, br) ppm (H_2O); 1.12 (t), 3.39 (q) ppm ($-OCH_2CH_3$). Absorption spectrum (THF) [λ_{max}, nm (ϵ, M^{-1} cm^{-1})]: 330 (4280), 422 (807) (sh).

Crystallography. Crystallographic data for complexes **1**, **2**, and **3** are summarized in Table 3 and in the Supporting Information. The crystals of **1**, **2**, and **3** are chunky. The crystals of **1**, **2**, **3** chosen for X-ray diffraction studies measured 0.10 × 0.10 × 0.06 mm, 0.45 × 0.25 × 0.16 mm, and 0.30 × 0.25 × 0.16 mm, respectively. Each crystal was mounted on a glass fiber. Diffraction measurements for complexes **1** and **3** were carried out at 150(1) K (293(2) K for complex **2**) on a Siemens SMART CCD diffractometer with graphite-monochromated Mo Kα radiation (λ 0.7107 Å) and θ between 1.25° and 25.00° for complex **1**, between 1.21° and 23.26° for complex **2**, and between 1.33° and 27.50° for complex **3**. Least-squares refinement of the positional and anisotropic thermal parameters for the contribution of all non-hydrogen atoms and fixed hydrogen atoms was based on F^2. A SADABS[21] absorption correction was made. The SHELXTL[22] structure refinement program was employed.

Crystallographic data (excluding structure factors) for the structures reported in this paper have been deposited with the Cambridge Crystallographic Data Centre: CCDC-177274, & CCDC-177275, and CCDC-186801. Copies of the data can be obtained free of charge on application to CCDC, 12 Union Road, Cambridge CB21EZ, U.K. (Fax: (+44)1223-336-033; E-mail: deposit@ccdc.cam.ac.uk.)

Acknowledgment. We gratefully acknowledge financial support from the National Science Council (Taiwan).

Supporting Information Available: Crystallographic data in CIF format. This material is available free of charge via the Internet at http://pubs.acs.org.

IC0261225

(21) Sheldrick, G. M. *SADABS, Siemens Area Detector Absorption Correction Program*; University of Göttingen: Göttingen, Germany, 1996.
(22) Sheldrick, G. M. *SHELXTL, Program for Crystal Structure Determination;* Siemens Analytical X-ray Instruments Inc.: Madison, WI, 1994.